Cerebrocerebellar Circuits for the Perceptual Cancellation of Eye-movement-induced Retinal Image Motion

Axel Lindner, Thomas Haarmeier, Michael Erb, Wolfgang Grodd, and Peter Thier

Abstract

■ Despite smooth pursuit eye movements, we are unaware of resultant retinal image motion. This example of perceptual invariance is achieved by comparing retinal image slip with an internal *reference signal* predicting the sensory consequences of the eye movement. This prediction can be manipulated experimentally, allowing one to vary the amount of self-induced image motion for which the reference signal compensates and, accordingly, the resulting percept of motion. Here we were able to map regions in CRUS I within the lateral cerebellar hemispheres that exhibited a significant correlation between functional magnetic resonance imaging signal amplitudes and the amount of motion predicted by the reference signal. The fact that these cerebellar regions were found to be functionally coupled with the left parieto-insular cortex and the supplementary eye fields points to these cortical areas as the sites of interaction between *predicted* and *experienced* sensory events, ultimately giving rise to the perception of a stable world despite self-induced retinal motion. ■

INTRODUCTION

Mobility complicates perception by violating the direct relationship between sensation and perception. Motion vision serves as a case in point. The retinal image motion an observer experiences is, in general, the result of the movement of the visual objects at which the observer is looking and movements of the observer's eyes relative to the external world. Vestibularly or optokinetically driven reflexes can be used to stabilize the eyes relative to the world in cases of inadvertent head movements, thereby minimizing self-induced retinal image motion. However, these reflexes must be shut down if an active reorientation based on eye, head, or body movements is needed. In such cases, perceiving the ''true'' visual motion of the world requires filtering out the self-induced components of image motion on the retina. For instance, during smooth pursuit eye movements (SPEM) this is accomplished by comparing the retinal signal with a *reference signal*, reflecting the visual action outcome (Helmholtz, 1962). Earlier studies assumed this reference signal to be a simple estimate of the eye movement, either based on an ''efference copy'' of the motor command (Helmholtz, 1962; Holst & Mittelstaedt, 1950), or on proprioceptive feedback from the actuators (Sherrington, 1918), or both (Bridgeman & Stark, 1991). However, the same eye movement may have different retinal consequences depending on the composition of the visual scene in terms of texture, luminance, color, and so forth. Thus, the reference signal of smooth pursuit cannot be established based on nonvisual, movement-related information only. Information about the visual context must supplement these nonvisual cues in order to come up with an accurate prediction of the expected visual consequences of the movement (Haarmeier, Bunjes, Lindner, Berret, & Thier, 2001. Also compare Crowell & Andersen, 2001; Wertheim, 1994).

Although we have developed a reasonable understanding of the functional principles allowing the maintenance of perceptual stability despite self-motion, we know surprisingly little about the underlying neural circuitry. Where is the prediction generated? And where does the comparison of reference signal predictions and retinal signals take place?

To address these questions, we aimed to map areas of the human brain, showing a specific correlation between reference signals and the blood oxygenation level dependent (BOLD) contrast. This required us to separate reference signal-evoked activity from other BOLD signals that are usually inextricably linked with the former: those triggered by the related eye movement and those evoked by the visual stimulus environment. Toward this end, we used the fact that reference signal predictions are continuously updated if a gross and consistent mismatch between the predicted and the actual visual consequences of the eye movement is simulated (Haarmeier

Hertie-Institut für Clinical Brain Research, Germany

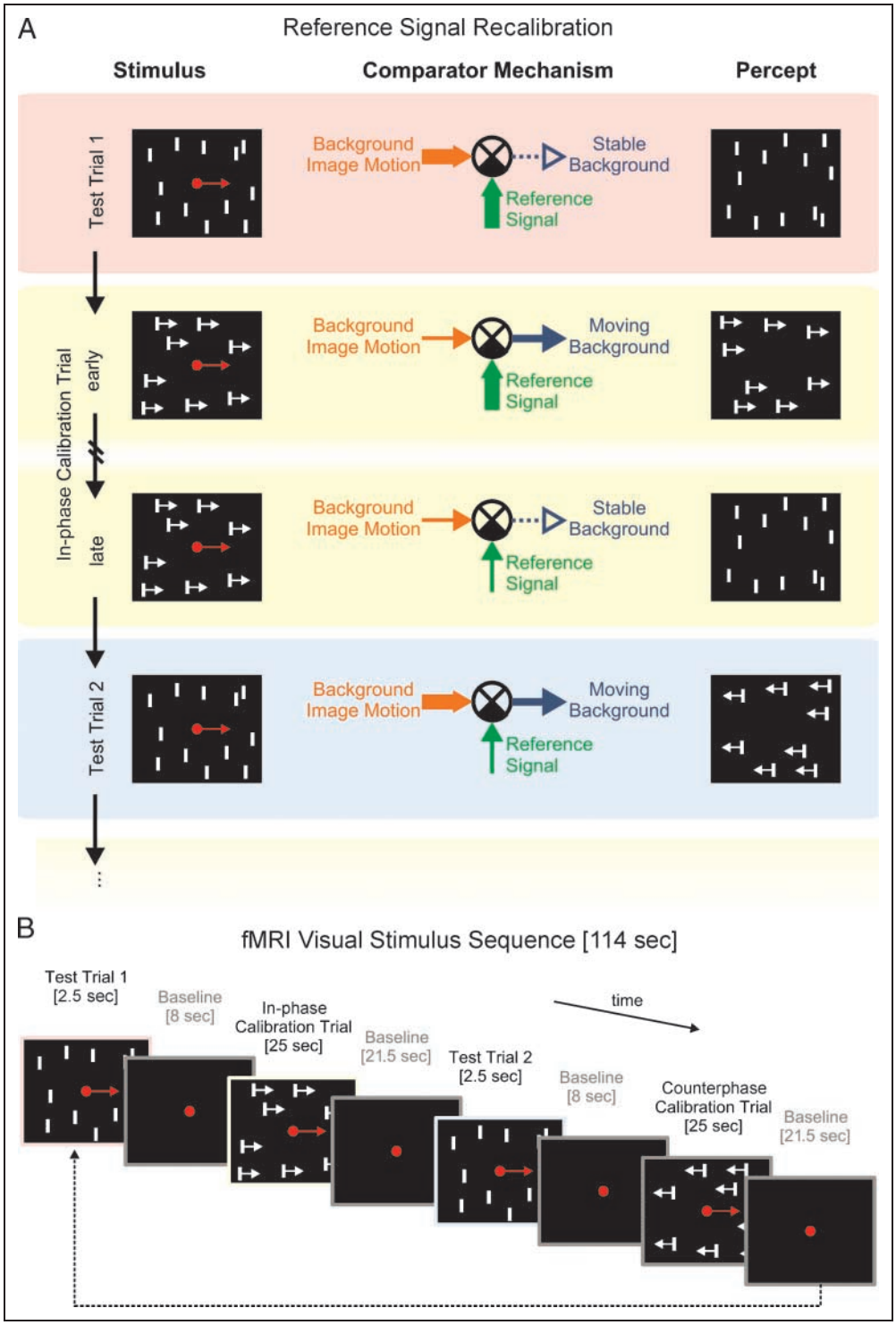

Figure 1. Reference signal recalibration and visual stimulation. (A) During pursuit over a structured background (Test Trial 1), an eye-movement-related reference signal (green arrow) usually compensates for pursuit-induced retinal image motion (orange arrow), and we therefore perceive a stationary background despite self-motion (dotted blue arrow). The actual "size" of each signal is reflected by the width of the arrows. If the background pattern is moved in the direction of the pursuit target (in-phase calibration trial), the amount of background image motion is reduced (thin orange arrow). Given the same eye movement as in the test trial, the reference signal predicts a greater amount of background image motion than actually sensed (early calibration, width of green arrow is identical to that of Test Trial 1). Due to this mismatch, the background pattern is perceived as moving (blue arrow). However, at the end of a long series of calibration cycles, the moving background will perceptually slow down and might finally appear as stationary (late calibration trial, dotted blue arrow). This change in motion perception is a consequence of a recalibration of the reference signal (thin green arrow; also refer to Haarmeier et al., 2001). Conversely, after recalibration, a stationary background will be perceived as moving (blue arrow in Test Trial 2). Hence, although being physically identical, Test Trials 1 and 2 are perceived differently due to changes of reference signal gain. (B) The visual stimulus sequence during fMRI consisted of two identical test trials, employing pursuit over a stationary structured background. Each test trial was preceded by one of two different calibration conditions, mimicking either a reference signal that is too small (counterphase calibration) or a reference signal that is too large (in-phase calibration). The fMRI stimulus sequence was repeated 14.5 times during one session, and two sessions were acquired for each of our subjects.

et al., 2001). Figure 1A gives an example of such a situation: Moving a large-field visual background in the same direction as the eyes (in-phase) reduces the actual amount of image flow as compared to the default situation, that is, smooth pursuit being carried out in a stationary environment. Thus, the amount of background image motion that is predicted by the reference signal is *too large* to equal the actual amount of image flow. If persistently confronted with such a discrepancy between reference signal predictions and actual image motion, the visual system decreases the "size" of the reference signal in order to dissolve this mismatch and to restore per-

ceptual stability (Haarmeier et al., 2001). That this is actually the case is demonstrated by the fact that occasional *test trials*, in which the visual background is kept stationary, give rise to the perception of background movement in the direction opposite to the eye movement.

By using this built-in *calibration mechanism*, we were able to vary the size of the reference signal for a given eye movement in a predictable manner while keeping the physical stimulus attributes identical. More importantly, this procedure enabled us to isolate reference-signal-related BOLD responses and to map a cerebrocerebellar circuit underlying the perceptual cancellation of smooth-pursuit-induced visual motion.

METHODS

Experimental Design

The actual visual stimulus sequence underlying our functional magnetic resonance imaging (fMRI) experiment is depicted in Figure 1B. The stimulus sequence contained two classes of trials serving complementary functions. fMRI test trials were used to evoke BOLD responses in conjunction with pursuit-induced retinal motion of a stationary background. These fMRI trials were embedded in calibration trials, which were needed in order to modify the expected visual consequences of self-motion in subsequent test trials.

Test trials engaged one cycle of sinusoidal smooth pursuit across an otherwise stationary background: The target guiding the eyes initially jumped either 6° to the left or to the right and remained at this position for 500 msec, providing subjects sufficient time to perform an initial saccade to foveate the target. Then it started moving smoothly toward the other side of the screen before finally returning to the starting position. Target motion for smooth pursuit followed a sinusoidal velocity profile with a maximal velocity of 15 deg/sec (0.4 cps, 12° amplitude; target size, 15 × 15 arcmin; 23 cd/m^2). Meanwhile, the pursuit target was presented on a visual background, consisting of white dot elements (maximum luminance, 115 cd/m^2; 15 × 15 arcmin; 3% dot density) displayed on the otherwise dark screen (1.7 cd/m^2; screen size, 15° × 12°). The luminance of the random dots was dynamically varied from 1.7 cd/m^2 (background luminance of the screen) to 115 cd/m^2 (maximum luminance) by multiplying it with the normalized square of the actual velocity of the pursuit target. In other words, at the turning points of the pursuit target no background pattern was visible (0% contrast), whereas its contrast was highest (97%) when the target passed through the center of the screen with maximum velocity. Thereby we guaranteed that the background pattern could only be perceived during ongoing eye movements but not around the turning points of the movement where eye velocity might reach zero and motion perception would possibly rely on visual signals only.

Reference signal-calibration trials used a series of 10 cycles of smooth pursuit in which the background moved consistently either in the direction of the eyes (in-phase) or opposite to the direction of the eyes (counterphase). The first variant mimicked the situation in which perception is determined by a reference signal that is too large in order to come up with the percept of a stable world; the second variant, the situation in which the reference signal is too small (compare Figure 1B). Maximum background speed was 10 deg/sec (0.4 cps, 8° amplitude) during in-phase and −5 deg/sec (0.4 cps, −4° amplitude) during counterphase calibration trials. Note that simulating such gross imperfections should in turn lead to a recalibration of the reference signal in order to ''optimize'' motion perception (compare Figure 1A; also refer to Haarmeier et al., 2001).

In order to instantly assess the size of the recalibrated reference signal we estimated the amount of background image motion for which the reference signal compensates: During one-half cycle of pursuit in a random position close to the end of the calibration trials (target cycle 8–9), the color of the pursuit target switched from red to magenta (and afterward back to red). This color cue caused our subjects to immediately judge and to remember the direction of perceived background motion. After the end of the calibration trial subjects then indicated the perceived direction by pressing one of two MRI-compatible buttons (25 mm distance between buttons) with their right thumb, indicating ''leftward'' and ''rightward'' decisions, respectively. No feedback was given. Such two-alternative forced choices were used to vary background movement velocity according to an adaptive staircase procedure (PEST; Lieberman & Pentland, 1982). This staircase procedure was used to identify the velocity of external horizontal background motion necessary to render the background perceptually stationary. At this point of subjective stationarity (PSS) the external velocity of the background cancels the component of pursuit-induced retinal image motion, which has not been compensated for by the reference signal, prompting subjects to vote in 50% of cases for either direction of motion. Accordingly, a PSS of 0 deg/sec reflects an ideal reference signal, which is able to fully compensate for pursuit-induced image motion, whereas a PSS corresponding to the velocity of the eyes (V_{pursuit}) indicates a complete lack of this signal. We used a reference signal gain (RS_{gain}) index to characterize the compensatory potential of the reference signal. It is given by Equation 1.

$$RS_{\text{gain}} = (V_{\text{pursuit}} - PSS)/V_{\text{pursuit}} \quad (1)$$

The aforementioned example of full compensation of self-induced image motion would correspond to a gain of 100%; the example of no compensation to a gain of 0%. Note that this measure of reference signal gain is

independent of differences in smooth pursuit performance, that is, eye velocity and/or pursuit direction. In order to estimate this gain in the two alternating calibration conditions (in-phase and counterphase), two independent staircase procedures according to the PEST algorithm were used in parallel. Both the background velocity and the related perceptual decision of each trial were subsequently entered into a post hoc probit analysis (McKee, Klein, & Teller, 1985) to obtain more precise estimates of the PSS, hence the reference signal gain within our individual subjects. Figure 2A shows an example of the psychophysical staircase procedures for a single subject and a single imaging session and the respective PSS values obtained by the probit analyses: Each staircase procedure converged at a certain amount of background motion, indicating a PSS of about 1 deg/sec in the counterphase calibration condition and a PSS of about 6 deg/sec in the in-phase calibration condition. Given the almost ideal pursuit performance of this subject ($V_{pursuit}$ ~15 deg/sec) the corresponding reference signal gain values would be about 90% and 60%, respectively. Despite alternating between the two different types of calibration, the perceptual interpretation of background motion for one particular calibration type (in-phase or counterphase) was remarkably constant over all trials of that type (see Figure 2A). Because the effects of calibration were not only consistent within but also across imaging sessions (paired t tests across sessions; in-phase calibration: $p = .21$, *ns*; counterphase calibration: $p = .73$, *ns*), we averaged PSS values across experiments to come up with a single estimate for each subject and for each type of calibration.

Finally, baseline conditions of different lengths (8 and 21.5 sec; compare Figure 1B) were presented interleaved with test and calibration trials. A long baseline trial always separated a reference signal calibration trial from the succeeding test trial. It ensured that the BOLD signals elicited by physically *identical* test trials would not overlap with the BOLD responses elicited by *different* calibration trials. The short baseline separated calibration trials from test trials. Baseline conditions comprised the response time for our subjects' behavior-

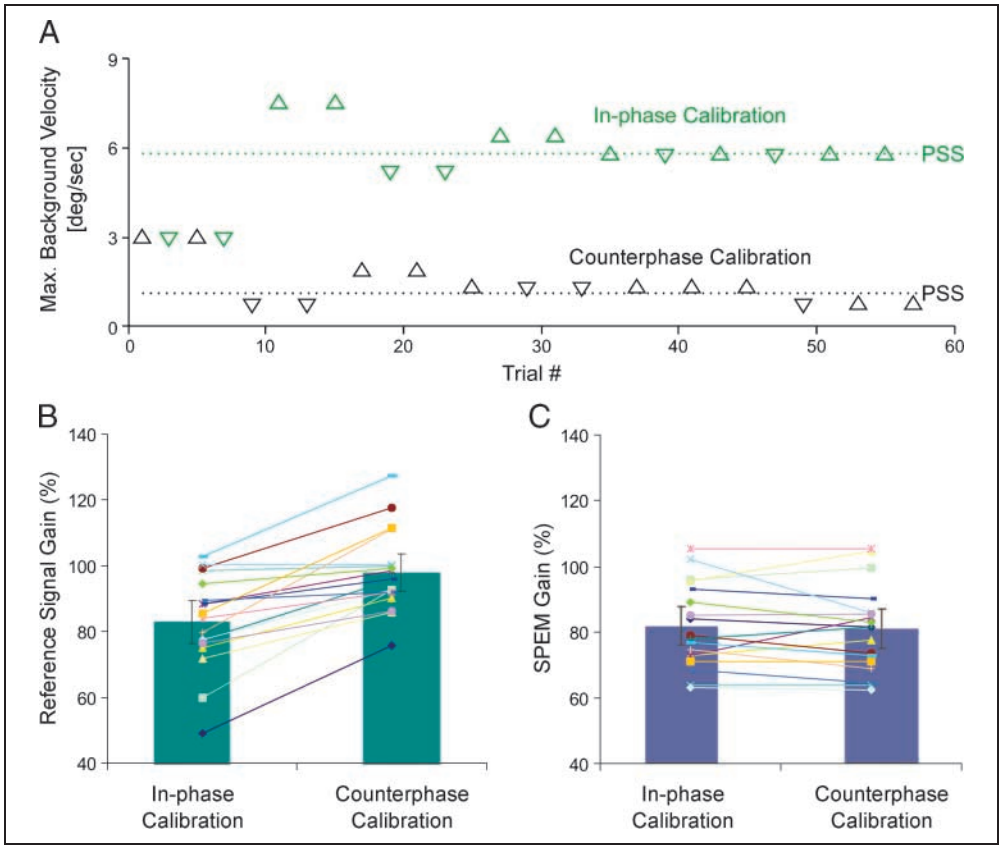

Figure 2. Behavioral measures during fMRI. (A) Point of subjective stationarity. The figure shows the perceptual decisions made by one subject during a single fMRI session: The subject's task was to indicate the perceived direction of background motion of a test pattern that was presented sometime at the end of each calibration trial. Upward triangles depict the subject's decision that the pattern moved in-phase with respect to the pursuit target; downward triangles denote counterphase decisions. The velocity of individual test patterns (positive velocities denote in-phase pattern motion) was governed by adaptive staircase procedures that converged at the point of subjective stationarity (PSS). At the PSS the subject perceived the test pattern as stationary and thus could no longer distinguish the direction of background motion. The subject had to guess. Two staircase procedures were run in parallel in order to estimate the PSS for both modes of calibration, in-phase (green triangles) and counterphase (black triangles). The broken lines indicate the respective PSS values, which were estimated by means of a probit analysis. Note that both staircase procedures nicely converged at the corresponding PSS, indicating stable reference signal recalibration despite alternating between the two modes of calibration. (B) Individual reference signal gains. The figure shows the reference signal gains of individual subjects at the end of the calibration procedure: When mimicking a reference signal that is too large (in-phase calibration), the gain in each individual subject became significantly smaller as compared to the counterphase calibration condition. The bars depict the respective group means ± 95% confidence intervals. (C) Individual and average gains of smooth pursuit eye movements (SPEM) during the test trials. Note that there was no significant difference between conditions.

al decision after calibration trials (6.5 sec; dark screen), the precalculation of the upcoming stimulus sequence (1 sec, dark screen), and an initial fixation period (7 sec prior to calibration trials and 14 sec prior to test trials). During the latter period the subjects' task was to fixate on a stationary red target (15 × 15 arcmin, 23 cd/m^2) presented in the center of an otherwise dark screen.

All visual stimuli were back-projected onto a translucent screen that subtended 15° × 12° by using a video projector (800 × 600 pixels, 60 Hz). Subjects viewed the visual stimuli via a mirror device that was mounted on the head coil of the MRI scanner (viewing distance, 1450 mm). An SGI workstation was used for stimulus generation as well as for registering our subjects' behavior.

Eye Movement Analysis

Horizontal eye movements were measured during the fMRI experiments by using an MRI-compatible infrared reflection eye tracker (Cambridge Research Systems, Rochester, UK). Eye position was sampled at 200 Hz and stored on the stimulus computer for later assessment of pursuit quality. Toward this end, we first applied a digital low-pass filter to the eye position records (cutoff frequency, 50 Hz), then calculated eye velocity and acceleration and detected saccades and eye blinks as described elsewhere (e.g., Lindner, Schwarz, & Ilg, 2001). Segments corresponding to saccades or eye blinks were removed from the eye velocity record. Finally, smooth pursuit gain was calculated for Test Trials 1 and 2 (compare Figure 1B) and for each subject by calculating the average ratio of eye to target velocity.

Subjects

Eighteen subjects, including one of the investigators (A.L.), participated in the experiments. All of them had normal or corrected-to-normal visual acuity. Subjects gave their written informed consent according to the declaration of Helsinki.

Imaging Procedures and Functional Image Analysis

A functional time series consisted of 550 gradient-echo planar imaging whole-brain scans (Siemens Vision 1.5T; Siemens AG, Erlangen, Germany), acquired every 3 sec (TE = 39 msec, FOV 192 × 192 mm^2, 64 × 64 matrix, 4 mm slice thickness, 1 mm gap, 3 × 3 × 4 mm^3 voxel size, 28 transversal slices). We ran two experiments per subject. The first 12 images of each experimental session were discarded to ensure that a steady-state magnetization had been reached. In addition, a T1-weighted data set (MPRAGE; TE = 4 msec, FOV 256 × 256 mm^2, 256 × 256 matrix, 1.5 mm slice thickness, 1.5 × 1 × 1 mm^3 voxel size, 128 sagittal slices) was collected to serve as an anatomical reference. For localizing activated voxels in the cerebellum, we referred to the 3-D atlas of the human cerebellum published by Schmahmann et al. (1999). Visual motion processing areas were identified based on the coordinates given by Sunaert, van Hecke, Marchal, and Orban (1999).

For image processing and statistical analysis, we used SPM99 (Wellcome Department of Cognitive Neurology, London, UK). Images of each subject were realigned by using the first scan as a reference. T1 anatomical images were coregistered to the mean image of the functional scans and then aligned to the SPM T1 template in the MNI space (Montreal Neurological Institute, mean brain). The calculated nonlinear transformation was applied to all images for spatial normalization. Finally the functional images were spatially smoothed with a Gaussian filter (8 × 8 × 12 mm^3 full width at half maximum). In addition, a high pass (cutoff period, 228 msec) and a low pass (canonical hemodynamic response function [HRF]) were used for temporal filtering.

Functional images were analyzed statistically by using a random effects model implemented into a two-level procedure. In a subject-specific analysis (first level), we specified a general linear model including four effects: two events corresponding to the test trials, which were modeled with a canonical HRF and its temporal derivative; and two blocks corresponding to the in-phase and counterphase calibration trials, modeled with a boxcar function, which was convolved with the HRF, and the temporal derivative. For each effect and for each subject a contrast image was calculated exhibiting the amplitude of the fitted BOLD response relative to the baseline condition. At the second level, test-trial-related contrast images were entered into a multiple regressions analysis (regressors: reference signal gain, smooth pursuit gain).

In addition, we performed connectivity analyses to map brain regions that are functionally coupled with reference-signal-related areas (Zald, Donndelinger, & Pardo, 1998). To this end, BOLD signal amplitudes of the test-trial-related contrast images were extracted in each relevant area: (1) for the voxel showing the maximum correlation with reference signal gain and (2) as the average amplitude calculated across the whole cluster of voxels, which showed significant correlation. We then mapped brain areas that significantly covaried with these ''activation profiles'' by means of a linear regressions analysis, which was calculated across the contrast images. In this and all the aforementioned analyses, we used a statistical threshold of $p < .05$ that was adjusted for multiple comparisons (corrected at cluster level; height threshold at voxel level, $p < .001$ uncorrected; extent threshold, $k > 20$ voxels; for details, see Friston, Holmes, Poline, Price, & Frith, 1996). The resulting areas as well as those obtained in our primary analysis were entered into a region-of-interest (ROI) analysis: For each individual ROI we again extracted the test-trial-related BOLD amplitudes from contrast images within those voxels, showing the local activation maximum according

to the mapping criteria. Next, each series of BOLD amplitudes was correlated with the related behavioral measures, reference signal gain, and pursuit gain, obtained for each individual subject and for each of the two physically identical test conditions.

RESULTS

We measured BOLD responses associated with the percept of visual motion induced by sinusoidal SPEM across a stationary large-field random dot pattern (test trials). Different perceptual interpretations of the resulting retinal image motion were achieved by modifying the size of the reference signal with which the retinal image motion signal was compared by means of calibration trials. Reference signal gain, on average, differed about 15% between conditions (compare Figure 2B; two-way ANOVA with the factors subject and conditions, significant main effects of subject, $p < .001$, and condition, $p < .001$). Reference signal gain was approximately 1 (98%) after counterphase calibration. Thus, a subsequently presented test trial was perceived as practically stationary (compare Test Trial 1 in Figure 1A). In the second condition (in-phase calibration) the gain averaged 83%, indicating that the compensation of pursuit-induced background motion was incomplete and an illusory eye-movement-induced background movement opposite to the direction of the eye movement was perceived during test trials (compare Test Trial 2 in Figure 1A). These differences in the size of the reference signal between the two conditions were not accompanied by any significant changes in mean pursuit eye velocity in test trials, although pursuit performance varied interindividually (two-way ANOVA with the factors subject and condition; significant main effect of subject, $p < .001$; effect of condition not significant). As shown in Figure 2C, mean eye velocity was about 80% of target velocity (i.e., ''SPEM gain''), independent of condition.

To identify brain areas in which activity reflected the perceptual as well as the interindividual behavioral differences, we looked for linear correlations between the BOLD signal and either the gains of the reference signal or smooth pursuit. First, we isolated the test-trial-related BOLD responses relative to the baseline condition separately for each subject and for each type of test trial. Regions of significant, test-trial-related activation were identified; these reflected the compound influences of visual, pursuit-related, as well as reference-signal-related processing. As exemplified by the horizontal sections cut through the visual cortex shown in Figure 3A, these test trials led to a highly significant BOLD response within distributed regions of the occipital and occipitotemporal cortex, including visual motion processing areas V1, V3a, and MT+. Other areas showing activation in this comparison lay in the premotor cortex, the frontal eye fields, the intraparietal cortex, and medial aspects of the prefrontal cortex (not shown in Figure 3A). In order to trace areas characterized by activity specifically related to the size of the reference signal (independent of smooth-pursuit gain and the size of the resulting retinal image motion), we subjected the individual contrast images to a multiple regressions analysis, with the reference signal gain as the first regressor and smooth-pursuit gain as the second regressor.

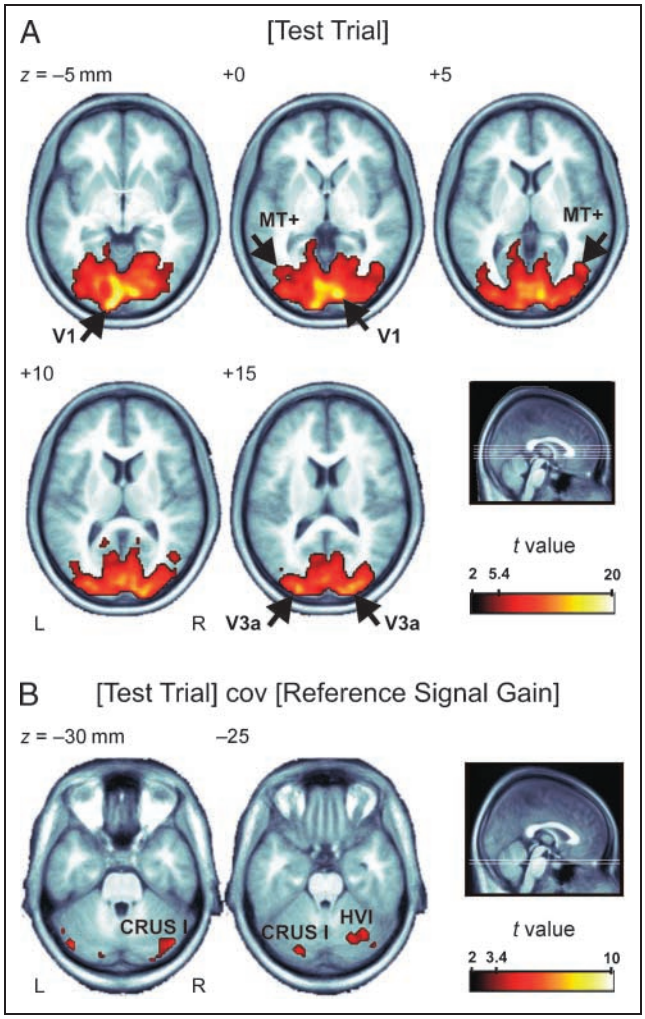

Figure 3. (A) Test-trial-related BOLD responses. The horizontal slices exhibit test-trial-related fMRI signal increases relative to the baseline condition within the occipital cortex. Arrows indicate motion-processing areas that were identified on the basis of the spatial localization of local activation maxima (see Methods). As in the following figures, functional images are overlaid onto the ''mean anatomy,'' calculated across subjects' normalized anatomical images. The sketch in the lower right corner indicates the height of the horizontal sections in a midsagittal section as well as a scale bar for the t values exhibited by the probability maps. The critical t value used as threshold criterion is indicated ($t = 5.4$). (B) Reference-signal-related BOLD responses. The horizontal slices display probability maps resulting from a negative correlation with reference signal gain ($p < .001$, uncorrected for multiple comparisons). The labeled areas are those that survived the statistical threshold criterion of $p < .05$ after correcting for multiple comparisons at cluster level.

Figure 3B depicts the two areas that showed a significant correlation ($p < .05$, corrected for multiple comparisons) with the reference signal. They were both localized in the cerebellum, corresponding to bilateral zones in CRUS I of the lateral hemispheres. The test-trial-related BOLD signal amplitudes of both areas were negatively correlated with the gain of the reference signal. Although the correlation maxima were confined to CRUS I, the cluster of significantly correlated voxels seemed to reach out toward CRUS II and the posterior vermis in the left and toward lobule HVI in the right cerebellar hemisphere. More importantly, these cerebellar activations could not be explained by interindividual differences in smooth pursuit gain and concomitant differences in retinal image slip because neither the activated zones in the cerebellum nor any other region of the brain showed any significant effect of pursuit gain on the BOLD response ($p > .05$, corrected for multiple comparisons). Moreover, the effect of the reference signal gain was independent of smooth-pursuit gain as indicated by the lack of a significant interaction between the two regressors.

In order to capture additional elements contributing to the inferential circuit determining motion perception during smooth pursuit (compare Figure 1A), we resorted to a functional connectivity analysis. By means of this analysis we mapped specific brain regions, showing BOLD responses covarying with those in the cerebellum, using CRUS I on either side as seeds (Zald et al., 1998). Table 1B summarizes all areas showing significant covariations with the cerebellar seeds. In short, activity of CRUS I covaried with both visual motion-related (V1, MT+, lingual gyrus [LG]; e.g., compare Sunaert et al., 1999) and pursuit-related areas (supplementary eye fields [SEFs], e.g., Petit & Haxby, 1999; pre-SEF, e.g., Lencer et al., 2004). Furthermore, regions within the middle and the inferior frontal gyri (MFG/IFG), the parieto-insular vestibular cortex (PIVC) and the cerebellum showed a significant correlation. To give an example, Figure 4 depicts all areas that were either positively (red) or negatively (blue) correlated with BOLD signal amplitudes within CRUS I of the right cerebellar hemisphere. Areas that showed a positive correlation were CRUS I of the left hemisphere, the representation of the peripheral visual field of area V1, the SEF, the pre-SEF, the posterior part of the middle frontal gyrus (BA 9), and the orbitofrontal part of the inferior temporal gyri. A negative correlation was obtained for the left parieto-insular cortex, probably corresponding to the PIVC (e.g., Bottini et al., 1994).

Finally, we examined whether or not BOLD responses in the cerebrocortical ROIs were percept related by subjecting the BOLD responses within these ROIs to a multiple regressions analysis with the two regressors RS and smooth pursuit gain. Table 1B summarizes the R values and the resulting levels of significance ($p < .05$ and $p < .01$, corrected for multiple comparisons). In addition, regions that had shown a significant correlation with the size of the reference signal in our primary multiple regressions analysis (Table 1A), as well as visual motion processing areas V1, V3a, and MT+ (Table 1C), were considered as controls. In short, as in our primary analysis, regions within CRUS I and the right HVI were significantly correlated with reference signal gain (see Figure 5A and B). The only cerebrocortical areas showing significant reference-signal/percept-related correlations were the left PIVC (Figure 5C) and the SEF (Figure 5D). CRUS II, the posterior vermis, prefrontal areas (IFG, MFG), and several visual motion processing areas (V1, V3a, MT+), the cuneus, and the lingual gyrus failed to show significant correlations. Finally, none of the ROIs explored showed a significant correlation with pursuit gain ($p > .05$, corrected for multiple comparisons; see Table 1).

DISCUSSION

The goal of our study was to map areas of the human brain that are involved in the perceptual cancellation of retinal image motion induced by SPEM. To this end, we systematically varied the gain of the eye-movement-related reference signal, which captured the expectation of the visual consequences of the eye movement and was removed from the actual retinal input to compensate for self-induced image motion. We found that the amplitude of the BOLD responses in corresponding parts of CRUS I of both lateral cerebellar hemispheres were significantly correlated with the amplitude of this eye-movement-related reference signal. These cerebellar regions were functionally coupled with several visual and eye-movement-related parietooccipital regions, prefrontal areas, and the left PIVC. Among these cerebrocortical regions, only the PIVC and the SEF exhibited a significant correlation with reference signal gain in an ROI analysis, whereas the ''classical'' visual motion processing areas and prefrontal regions did not show such a dependency.

Methodological Considerations and Limitations

Can it be taken for granted that BOLD responses within the cerebellum reflect the smooth pursuit-related reference signal? A possible concern might be that these responses are shaped by putative differences in task-related motor behavior, differences in the properties of the visual stimuli presented, sensory adaptation (e.g., a motion aftereffect), or differences in the attentional load. We are confident that relevant differences in these variables can be ruled out because our experimental paradigm was specifically designed to vary reference signal gain and the resulting percept of motion, while keeping eye movements, retinal image slip, as well as attentional and general task loads constant. BOLD responses were analyzed for test trials, which

Table 1. ROI Analysis

Brain Area	*x, y, z [mm MNI]*	*r RS_{gain}*	*r SPEM Gain*	*Coupling*
(A) Cerebellar areas significantly correlated with RS_{gain}				
CRUS I right	45, −75, −30	−.591**	.100	l, L, –, –
CRUS I left	−24, −84, −20	−.511*	−.094	–, L, –, r
	−42, −75, −30	−.477*	−.061	l, –, –, –
HVI right	24, −69, −25	−.481*	−.182	–, –, –, –
	36, −66, −25	−.611**	.266	–, –, R, –
(B) Cerebrocortical areas functionally correlated with CRUS I				
LG	12, −60, −5	−.392	.282	–, –, R, –
	18, −72, −5	−.248	.433	–, –, R, –
V1 right	9, −81, 5	−.435	.300	l, –, –, r
V1 left	−6, −81, 0	−.269	.249	l, –, –, r
Cuneus	−6, −96, 25	−.280	.434	–, –, R, –
MT+/IFG right	57, −66, −10	−.370	.042	l, L, –, –
SEF/SMA	6, 15, 70	−.476*	.172	l, –, –, r
	3, 24, 65	−.419	−.030	l, L, –, –
Pre-SMA	3, 39, 60	−.354	−.081	–, –, –, r
	3, 27, 65	−.421	−.061	–, –, –, r
	0, 30, 55	−.358	−.073	l, –, –, –
MFG right (*ns*)	45, 24, 50	−.285	.036	–, –, –, r
MFG left	−42, 21, 45	−.281	.056	–, –, –, r
IFG right	48, 39, −15	−.392	.043	–, –, –, r
IFG left	−48, 24, −15	−.213	−.110	–, –, –, r
PIVC left	−39, −21, 10	.477*	−.391	–, –, R, –
(C) Controls: Visual motion processing areas				
V1 right	9, 90, 0	−.071	.265	
V1 left	−9, −99, −5	−.083	.021	
V3a right	24, −93, 15	−.202	.123	
V3a left	−24, −96, 15	.010	.187	
MT+ right	48, −66, 5	−.142	.410	
MT+ left	−39, −69, 0	−.007	.101	

LG= lingual gyrus; IFG = inferior frontal gyrus; SEF = supplementary eye field; SMA = supplementary motor area; MFG = middle frontal gyrus; PIVC = parieto-insular vestibular cortex.

The table shows the results of the ROI analysis. The mean BOLD signal amplitude of each ROI was correlated with reference signal gain (RS_{gain}) and smooth pursuit gain (SPEM gain). For each ROI, the results of the regression analyses (*R* values) and the exact anatomical location according to the MNI space (see Methods) are given. (A) Regions significantly activated in our primary regressions analysis served as controls. (B) Cerebrocortical regions that were functionally coupled with CRUS I on either side. Coupling indices refer to areas that significantly covaried with BOLD signals from CRUS I of the right (r, R) or left (l, L) cerebellar hemisphere. BOLD signal amplitudes were extracted either for the voxel showing the maximum correlation with reference signal gain (l, r) or for the whole cluster of activated voxels (L, R). (C) Visual motion processing areas as depicted in Figure 3A served as further controls for the ROI analyses.

*$p < .05$, corrected for multiple comparisons.

**$p < .01$, corrected for multiple comparisons.

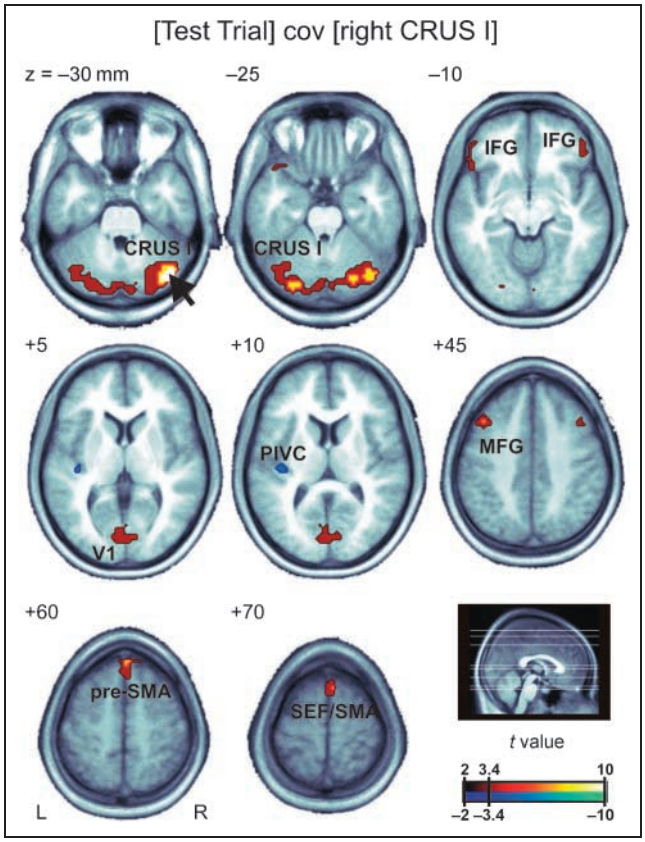

Figure 4. Areas functionally correlated with CRUS I. The slices exhibit brain regions that covary positively (red) or negatively (blue) with activity within CRUS I (see arrow) of the right cerebellar hemisphere ($p < .001$, uncorrected for multiple comparisons). Other conventions are as in Figure 3.

were physically identical, differing only in the percept of eye-movement-induced visual motion. Not only pursuit-target velocity but also smooth-pursuit gain and thus pursuit-induced retinal background motion was indeed the same in these conditions. The differences in the percept of background motion were evoked by embedding test trials in specific sets of calibration trials that should change the size of the reference signal. It is important to emphasize that subjects were instructed not to come up with judgments on the direction of perceived background movement for test trials to avoid BOLD responses due to the indicative behavior. Rather, decisions on the direction of background movement were confined to the end of calibration trials. One remaining concern might be that the calibration stimuli may have caused motion adaptation rather than changing the size of the reference signal. However, this concern can be dispelled. All trials were motion balanced because background motion was presented in alternating directions within each trial, thus zeroing its adaptive potential. We have previously shown that despite such motion-balanced designs the perceptual interpretation of self-induced motion can be altered by recalibrating the reference signal, although no motion aftereffect of a background pattern during stationary fixation is present (see Haarmeier et al., 2001). In the same study, we further demonstrated that such recalibration of smooth pursuit-related reference signals occurs independently for leftward and rightward eye movements—a finding that cannot be explained by sensory aftereffects. Finally, if the changes in perception, which we attributed to changes in reference signal gains, were simply artifacts of a rather unspecific desensitization to visual motion, we would expect to see percept-related (i.e., reference signal related) BOLD responses in area MT+, a structure known to be involved in mediating the motion aftereffect (e.g., see Huk, Ress, & Heeger, 2001). This was not the case. We are thus confident that the experimental design chosen ensured that we specifically mapped areas of the human brain related to the eye-movement-related reference signal.

Our method did not allow us, however, to distinguish whether the respective fMRI signals were related to the plasticity of a corollary discharge of the eye movement motor commands (Sperry, 1950) and/or proprioception, ultimately being used to predict the sensory action outcome or, alternatively, to the plasticity of the latter prediction itself. Furthermore, our method cannot separate reference-signal-related from percept-related fMRI activity: If the reference signal changes, the percept also must change. Thus, the reference-signal-related BOLD signal in the cerebellum might likewise be interpreted as reflecting percept-related processing. Although this possibility cannot be ruled out with any certainty, we do not consider it to be likely, given the huge amount of evidence implicating the cerebral cortex in visual awareness and consciousness in general, rather than subcortical structures such as the cerebellum. This view is, for instance, supported by patient R.W. (Haarmeier, Thier, Repnow, & Petersen, 1997), who shows a specific deficit in the perceptual cancellation of pursuit-induced image motion due to bilateral lesions involving large parts of the extrastriate and parietal cortex while sparing V1 and the cerebellum. On the one hand, the absence of reference signal-related activity in the cerebral cortex most probably reflects the insufficient sensitivity of the analysis employed, rather than a lack of an involvement of the cerebral cortex in the conscious perception of visual motion. On the other hand, the role of the cerebellum in motion perception is most probably an indirect one, namely, to provide and/or optimize eye-movement-related reference signals.

Cerebellar Regions Involved in the Cancellation of Self-induced Image Motion

Only cerebellar regions within the lateral parts of the hemispheres showed a significant correlation with reference signal gain. The clusters of significantly activated voxels were located in CRUS I on either side, making

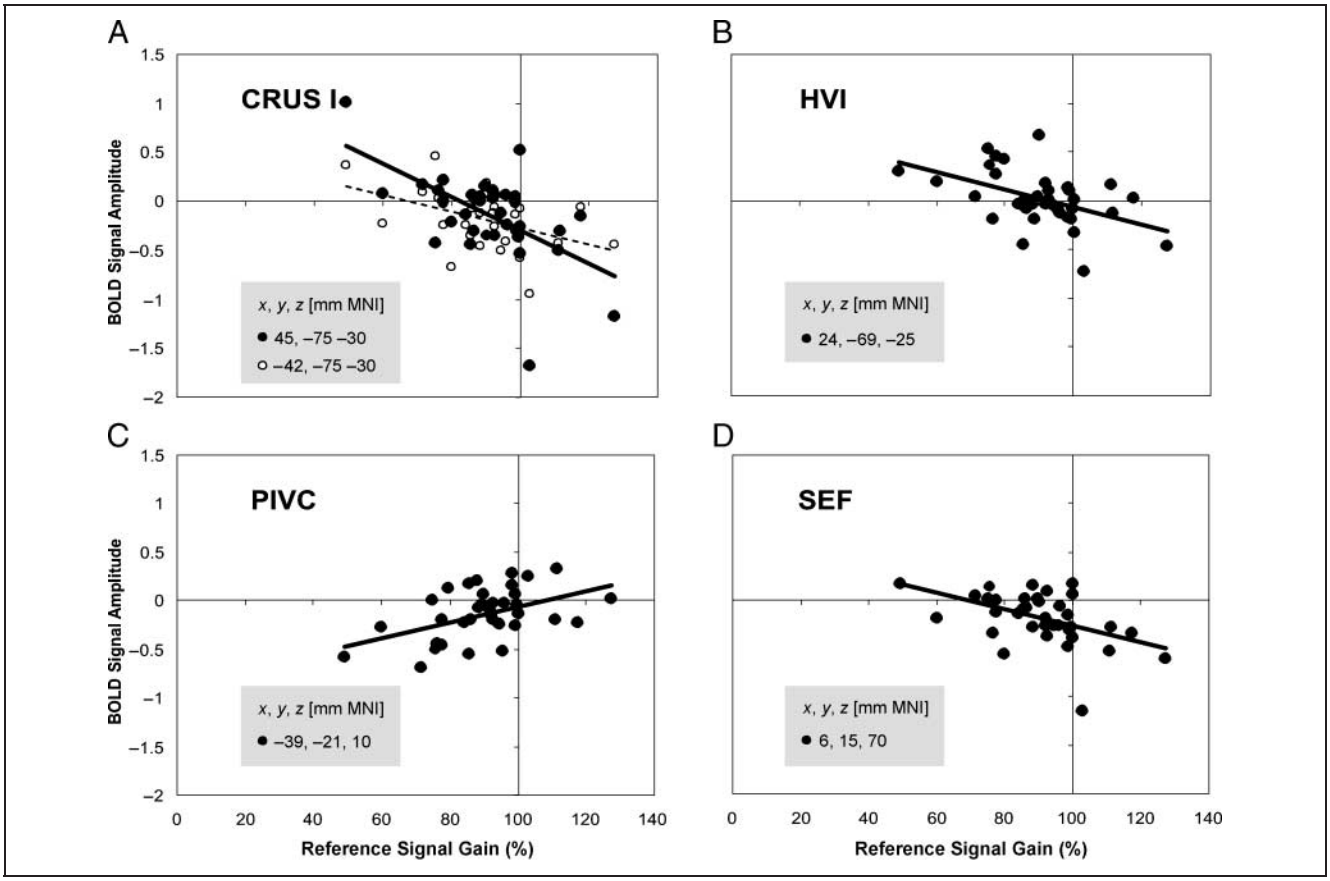

Figure 5. ROI analysis. The graphs plot the BOLD signal amplitude of different ROIs as a function of reference signal gain. Lines represent the linear fit to the data (left hemisphere, broken line; right hemisphere, solid line).

encroachments on CRUS II and the posterior vermis in the left and lobule HVI in the right hemisphere. Corresponding parts of the lateral cerebellum have been shown to contain vision- and eye-movement-related neurons in monkeys (Marple-Horvat & Stein, 1990) and electrical stimulation in the same regions elicits saccades as well as SPEM (Ron & Robinson, 1973). Also in humans, functional activations of CRUS I and its neighboring lobules have been previously described in several imaging studies engaging eye movements. For instance, Konen, Kleiser, Seitz, and Bremmer (2005) and Tanabe, Tregellas, Miller, Ross, and Freedman (2002) found an activation of these parts of the lateral cerebellar hemispheres when analyzing BOLD contrasts between smooth pursuit versus stationary fixation. A bilateral activation of this part of the cerebellum was also described in conjunction with optokinetic nystagmus (OKN), OKN suppression, and saccadic eye movements (Dieterich, Bucher, Seelos, & Brandt, 2000).

However, none of the aforementioned studies allows attributing a functional role to CRUS I, CRUS II, or HVI: Even though it is emphasized that these regions might be involved in generating eye movements, they may likewise just participate in the processing of visual information related to the (upcoming or actual) movement. Moreover, it may be worth considering the function emphasized by the present report: namely, the generation of reference signals needed for the optimization of vision. In fact, CRUS I seems to maintain an anatomical position ideal for integrating visual and nonvisual signals needed to generate and/or optimize a reference signal, reflecting the visual consequences of an eye movement. Input to this region arises from several parietooccipital and frontal areas involved in the processing of visual motion and eye-movement-related information such as areas MT, MST, LIP, FEF, and SEF. These areas strongly project to dorsolateral and dorsomedial pontine nuclei (Shook et al., 1990; Glickstein et al., 1980; Brodal, 1978), which in turn send efferences to the dorsal paraflocculus, the posterior vermis, and to also other parts of the cerebellum, including lobule CRUS I (Glickstein et al., 1994; Brodal, 1979). A second important source of eye-movement-related input, especially from the frontal cortex, is the nucleus reticularis tegmenti pontis, which among others also projects to CRUS I (Brodal, 1979). Finally, previous electrophysiological work (Sasaki, Oka, Kawaguchi, Jinnai, & Yasuda, 1977; Sasaki, Kawaguchi, Oka, Sakai, & Mizuno, 1976) suggests that CRUS I might feed back on the same areas from which it receives its input.

Thus, the lateral cerebellar hemisphere seems to be an ideal candidate structure for processing eye-movement-related reference signals and for conveying this signal to an inferential cerebrocerebellar circuit determining the visual percept.

Cerebrocerebellar Circuits for the Cancellation of Self-induced Image Motion

To detect the putative cerebrocerebellar circuit, which interacts with reference signals in the cerebellum, we took a two-step approach. In the first step, we delineated cerebrocortical areas showing BOLD responses covarying with those in cerebellar CRUS I. In the second step, we isolated areas showing a specific correlation with reference signal gain among these ROIs. The areas extracted by this approach were the left and the right SEF as well as the left PIVC. In addition, parietooccipital as well as prefrontal areas exhibited BOLD responses covarying with those in CRUS I. However, these regions did not show a link to the reference signal. Instead they might serve as sources of visual and oculomotor information for CRUS I needed for the generation of the eye movement reference signal. Alternatively, some of these areas might receive information not relevant for the percept of motion. Unfortunately, the functional connectivity analysis does not allow us to distinguish between these possibilities. It reveals communication, but it is not able to infer causal relationships: We are not able to distinguish whether covariation reflects the fact that a specific cerebral region sends signals to the cerebellum, receives input from the cerebellum, maintains information exchange in both directions, or receives common input. Fortunately, we could at least examine whether a cerebrocortical region of interest showed percept-related activity.

The SEF, one of the two areas that showed reference-signal-related BOLD responses, was originally identified by Schlag and Schlag-Rey (1987) in monkeys as a part of the supplementary motor cortex (SMA), contributing to the generation of saccadic eye movements. Later work showed that the SEF is also involved in smooth pursuit (Heinen, 1995). Like neurons in other parts of the SMA, those in the SEF usually start firing some hundred milliseconds before the motor act (Schlag & Schlag-Rey, 1987). This is true also for pursuit-related neurons that fire in anticipation of changes in target motion (Heinen & Liu, 1997) and facilitate predictive pursuit when stimulated electrically (Missal & Heinen, 2004). Similar observations have been obtained in human imaging studies showing increases in BOLD amplitudes within the areas SEF, SMA, and pre-SMA, which are related to the predictability of target motion during smooth pursuit (Konen et al., 2005; Schmid, Rees, Frith, & Barnes, 2001). Thus, the SEF seems to form a processing stage in motor planning that prepares an upcoming goal-directed motor act. By the same token, the SEF might contribute to set up an eye-movement-related reference signal, predicting the sensory consequences of actions. This interpretation is supported by the fact that transcranial magnetic stimulation of the SMA virtually abolishes the perceptual cancellation of self-induced somatosensory stimuli (Haggard & Whitford, 2004). As the SEF and the SMA share many general functional properties, this finding might generalize to the eye-movement-related part of the SMA as well. One speculative interpretation of the functional coupling between the SMA and CRUS I could therefore be that it is the SMA that provides a first, still crude sketch of the reference signal that is continuously updated on a short timescale by the cerebellum.

The second cerebrocortical region showing a covariation with CRUS I as well as reference-signal-related activity was a patch of left parieto-insular cortex, largely congruent with the putative human homologue of the PIVC (e.g., Bottini et al., 1994). PIVC was first described in monkeys as a primarily vestibular region. However, neuronal activity within this area can also be modulated by optokinetic and somatosensory stimuli (for a review, see Guldin & Grüsser, 1998). Monkey PIVC receives direct and indirect input from several cerebrocortical areas processing visual motion, namely, areas MST, V3a, V6, visual posterior sylvian (VPS), and area 7a (Galletti & Fattori, 2003; Guldin & Grüsser, 1998; Shipp, Blanton, & Zeki, 1998). Interestingly, all of these regions projecting to the PIVC contain neurons that can distinguish eye-movement- and object-induced image motion (e.g., V3a: Galletti, Battaglini, & Fattori., 1990; V6: Galletti & Fattori, 2003; 7a: Sakata, Shibutani, Kawano, & Harrington, 1985; MST: Thier & Erickson, 1992; VPS: Thier, Haarmeier, Chakraborty, Lindner, & Tikhonov, 2001). Similar to monkey PIVC, the putative human homologue can also be driven by vestibular as well as by optokinetic stimuli (Dieterich, Bense, Stephan, Yousry, & Brandt, 2003). Adding visual and vestibular information about self-movement and eventually reference-signal-related information received via its interconnection with premotor cortex (Guldin, Akbarian, & Grusser, 1992), the PIVC seems to be an ideal candidate to elaborate an allocentric frame of reference for the perceptual interpretation of visual motion information. This view is supported by a recent fMRI study (Kleinschmidt et al., 2002), in which subjects viewed a rotating windmill pattern that induced a bistable percept: Subjects either perceived a rotating mill or, alternatively, they experienced self-motion (circular vection). BOLD responses of the PIVC clearly distinguished between these two conditions by covarying with the perception of motion in world-centered coordinates (Kleinschmidt et al., 2002; Thilo, Probst, Bronstein, Ito, & Gresty, 1999). Our findings suggest not only that the PIVC exhibits percept-related activity, but that, more specifically, the PIVC seems to represent the processing stage at which the cancellation of self-induced image motion takes place. This is indicated by

the fact that the stronger the active compensation of visual motion energy (i.e., the larger the reference signal gain) the stronger the BOLD response within the PIVC (compare Figure 5C).

Human motion processing area MT+, the putative homologue of monkey area MT/MST, did not show reference-signal-related activity in our study. This is in line with previous electroencephalogram (Haarmeier & Thier, 1998) and magnetoelectroencephalogram (Tikhonov, Haarmeier, Thier, Braun, & Lutzenberger, 2004) studies. In these electrophysiological studies, using an experimental approach very similar to the one described here, electric and magnetic responses evoked by pursuit-induced retinal image motion attributed to MT+ did not show a dependency on the reference signal. A noteworthy point of difference between our results and previous work relates to the already mentioned study of Tikhonov et al. (2004). In that study, reference-signal-related evoked magnetic fields were attributed to a single equivalent current dipole located on the medial aspect of the parietooccipital cortex (PO), absent in the present investigation. Interestingly, the same region was shown to be activated in a previous positron emission tomography study, in which the amount of perceived circular vection induced by a rotating structured background was correlated with cerebral blood flow (Brandt, Bartenstein, Janek, & Dieterich, 1998). Moreover, this latter study demonstrated an inverse interaction between PO and the PIVC during the perception of self-rotation. The lack of activation of PO in our study could be due to differences in stimulus size (Previc, Liotti, Blakemore, Beer, & Fox, 2000): Both Tikhonov et al. (2004) and Brandt et al. (1988) used visual stimuli considerably larger (~900% and ~1700%, respectively) than the visual background employed here.

The Role of the Cerebellum and Its Interaction with Cerebrocortical Areas

Our conclusion that the cerebellum influences the processing of sensory information by providing a sensory expectation is not without precedent. As established by Bell (2001), the cerebellar-like structure of weakly electric fishes compares a prediction of the expected and the actual sensory consequences of self-produced electrical fields. Such fields are generated by the animal and analyzed by an elaborate electrosensory system in order to filter out behaviorally relevant distortions of their own electric field caused by the environment (for a review, see Bell, 2001). Similarly, a comparable role of the cerebellum may also contribute to our ability to distinguish between external and self-produced tactile stimulation (Blakemore, Wolpert, & Frith, 1998). More specifically, Blakemore, Frith, and Wolbert (2001) suggested that the cerebellum might convey an error signal reflecting the discrepancy between predicted and actually sensed tactile information. The negative correlation of reference signal gains and cerebellar BOLD signals in our study supports this view: The smaller the reference signal gain and thus the larger the sensory prediction error, the larger the cerebellar fMRI response (compare Figure 5A and B). Such a verification of internal predictions about how motor behavior influences sensation could even help to improve perception, a notion that offers a conciliatory interpretation of the controversial nonmotor functions of the cerebellum. The cerebellum has sensory, perceptual, and other kinds of nonmotor functions because it internalizes intricate ''knowledge'' of motor behavior (Ito, 2005). This knowledge is not only used to fine-tune movements (Imamizu et al., 2000; Barash et al., 1999), but also to assess the widespread nonmotor consequences of behavior. Specifically, our findings imply that CRUS I of the lateral cerebellum integrates visual and nonvisual information about the eye movement to optimize reference signals, capturing the expectation of the visual consequences of SPEM. These reference signals probably originate in the supplementary eye fields and are eventually relayed to the PIVC. Neurons in the latter cortical area may allow us to cancel out the visual consequences of ego motion in order to isolate visual motion signals originating from the environment.

Acknowledgments

This work was made possible by grants from the Human Frontier Science Organization (RGP 0023/2001-B), the Volkswagen Foundation (1/80 727) and the Deutsche Forschungsgemeinschaft (SFB 550 and Graduiertenkolleg Kognitive Neurobiologie). We thank Asha Iyer and Karen Bauer for correcting the manuscript.

Reprint requests should be sent to Peter Thier or Alex Lindner, Hertie-Institute for Clinical Brain Research, Department of Cognitive Neurology, Hoppe-Seyler-Str. 3, 72076 Tübingen, Germany, or via e-mail: thier@uni-tuebingen.de or alindner@caltech.edu.

REFERENCES

Barash, S., Melikyan, A., Sivakov, A., Zhang, M., Glickstein, M., & Thier, P. (1999). Saccadic dysmetria and adaptation after lesions of the cerebellar cortex. *Journal of Neuroscience, 19,* 10931–10939.

Bell, C. C. (2001). Memory-based expectations in electrosensory systems. *Current Opinion in Neurobiology, 11,* 481–487.

Blakemore, S.-J., Frith, C. D., & Wolpert, D. M. (2001). The cerebellum is involved in predicting the sensory consequences of action. *NeuroReport, 12,* 1879–1884.

Blakemore, S.-J., Wolpert, D. M., & Frith, C. D. (1998). Central cancellation of self-produced tickle sensation. *Nature Neuroscience, 1,* 635–640.

Bottini, G., Sterzi, R., Paulesu, E., Vallar, G., Cappa, S. F., Erminio, F., et al. (1994). Identification of the central vestibular projections in man: A positron emission tomography activation study. *Experimental Brain Research, 99,* 164–169.

Brandt, T., Bartenstein, P., Janek, A., & Dieterich, M. (1998). Reciprocal inhibitory visual–vestibular interaction. Visual motion stimulation deactivates the parieto-insular vestibular cortex. *Brain, 121,* 1749–1758.

Bridgeman, B., & Stark, L. (1991). Ocular proprioception and efference copy in registering visual direction. *Vision Research, 31,* 1903–1913.

Brodal, P. (1978). The corticopontine projection in the rhesus monkey: Origin and principles of organization. *Brain, 101,* 251–283.

Brodal, P. (1979). The pontocerebellar projection in the rhesus monkey: An experimental study with retrograde axonal transport of horseradish peroxidase. *Neuroscience, 4,* 193–208.

Crowell, J. A., & Andersen, R. A. (2001). Pursuit compensation during self-motion. *Perception, 30,* 1465–1488.

Dieterich, M., Bense, S., Stephan, T., Yousry, T. A., & Brandt, T. (2003). fMRI signal increases and decreases in cortical areas during small-field optokinetic stimulation and central fixation. *Experimental Brain Research, 148,* 117–127.

Dieterich, M., Bucher, S. F., Seelos, K. C., & Brandt, T. (2000). Cerebellar activation during optokinetic stimulation and saccades. *Neurology, 54,* 148–155.

Friston, K. J., Holmes, A., Poline, J.-B., Price, C. J., & Frith, C. D. (1996). Detecting activations in PET and fMRI: Levels of inference and power. *Neuroimage, 40,* 223–235.

Galletti, C., Battaglini, P. P., & Fattori, P. (1990). 'Real-motion' cells in area V3A of macaque visual cortex. *Experimental Brain Research, 82,* 67–76.

Galletti, C., & Fattori, P. (2003). Neuronal mechanisms for detection of motion in the field of view. *Neuropsychologia, 41,* 1717–1727.

Glickstein, M., Cohen, J. L., Dixon, B., Gibson, A., Hollins, M., Labossiere, E., et al. (1980). Corticopontine visual projections in macaque monkeys. *Journal of Comparative Neurology, 190,* 209–229.

Glickstein, M., Gerrits, N., Kralj-Hans, I., Mercier, B., Stein, J., & Voogd, J. (1994). Visual pontocerebellar projections in the macaque. *Journal of Comparative Neurology, 349,* 51–72.

Guldin, W. O., Akbarian, S., & Grusser, O. J. (1992). Cortico-cortical connections and cytoarchitectonics of the primate vestibular cortex: A study in squirrel monkeys (*Saimiri sciureus*). *Journal of Comparative Neurology, 326,* 375–401.

Guldin, W. O., & Grüsser, O.-J. (1998). Is there a vestibular cortex? *Trends in Neuroscience, 21,* 254–259.

Haarmeier, T., Bunjes, F., Lindner, A., Berret, E., & Thier, P. (2001). Optimizing visual motion perception during eye movements. *Neuron, 32,* 527–535.

Haarmeier, T., & Thier, P. (1998). An electrophysiological correlate of visual motion awareness in man. *Journal of Cognitive Neuroscience, 10,* 464–471.

Haarmeier, T., Thier, P., Repnow, M., & Petersen, D. (1997). False perception of motion in a patient who cannot compensate for eye movements. *Nature, 389,* 849–852.

Haggard, P., & Whitford, B. (2004). Supplementary motor area provides an efferent signal for sensory suppression. *Cognitive Brain Research, 19,* 52–58.

Heinen, S. J. (1995). Single neuron activity in the dorsomedial frontal cortex during smooth pursuit eye movements. *Experimental Brain Research, 104,* 357–361.

Heinen, S. J., & Liu, M. (1997). Single-neuron activity in the dorsomedial frontal cortex during smooth-pursuit eye movements to predictable target motion. *Visual Neuroscience, 14,* 853–865.

Huk, A. C., Ress, D., & Heeger, D. J. (2001). Neuronal basis of the motion aftereffect reconsidered. *Neuron, 32,* 161–172.

Imamizu, H., Miyauchi, S., Tamada, T., Sasaki, Y., Takino, R., Putz, B., et al. (2000). Human cerebellar activity reflecting an acquired internal model of a new tool. *Nature, 403,* 192–195.

Ito, M. (2005). Bases and implications of learning in the cerebellum—Adaptive control and internal model mechanism. *Progress in Brain Research, 148,* 95–109.

Kleinschmidt, A., Thilo, K. V., Büchel, C., Gresty, M. A., Bronstein, A. M., & Frackowiak, S. J. (2002). Neural correlates of visual-motion perception as object- or self-motion. *Neuroimage, 16,* 873–882.

Konen, C. S., Kleiser, R., Seitz, R. J., & Bremmer, F. (2005). An fMRI study of optokinetic nystagmus and smooth-pursuit eye movements in humans. *Experimental Brain Research, 165,* 203–216.

Lencer, R., Nagel, M., Sprenger, A., Zapf, S., Erdmann, C., Heide, W., et al. (2004). Cortical mechanisms of smooth pursuit eye movements with target blanking. An fMRI study. *European Journal of Neuroscience, 19,* 1430–1436.

Lieberman, H. R., & Pentland, A. P. (1982). Microcomputer-based estimation of psychophysical thresholds: The best PEST. *Behavior Research Methods & Instruments, 14,* 21–25.

Lindner, A., Schwarz, U., & Ilg, U. J. (2001). Cancellation of self-induced retinal image motion during smooth pursuit eye movements. *Vision Research, 41,* 1685–1694.

Marple-Horvat, D. E., & Stein, J. F. (1990). Neuronal activity in the lateral cerebellum of trained monkeys, related to visual stimuli or to eye movements. *Journal of Physiology, 428,* 595–614.

McKee, S. P., Klein, S. A., & Teller, D. Y. (1985). Statistical properties of forced choice psychometric functions: Implications of probit analysis. *Perception and Psychophysics, 37,* 286–298.

Missal, M., & Heinen, S. J. (2004). Supplementary eye fields stimulation facilitates anticipatory pursuit. *Journal of Neurophysiology, 92,* 1257–1262.

Petit, L., & Haxby, J. V. (1999). Functional anatomy of pursuit eye movements in humans as revealed by fMRI. *Journal of Neurophysiology, 82,* 463–471.

Previc, F. H., Liotti, M., Blakemore, C., Beer, J., & Fox, P. (2000). Functional imaging of brain areas involved in the processing of coherent and incoherent wide field-of-view visual motion. *Experimental Brain Research, 131,* 393–405.

Ron, S., & Robinson, D. A. (1973). Eye movements evoked by cerebellar stimulation in the alert monkey. *Journal of Neurophysiology, 36,* 1004–1022.

Sakata, H., Shibutani, H., Kawano, K., & Harrington, T. L. (1985). Neural mechanisms of space vision in the parietal association cortex of the monkey. *Vision Research, 25,* 453–463.

Sasaki, K., Kawaguchi, S., Oka, H., Sakai, M., & Mizuno, N. (1976). Electrophysiological studies on the cerebellocerebral projections in monkeys. *Experimental Brain Research, 24,* 495–507.

Sasaki, K., Oka, H., Kawaguchi, S., Jinnai, K., & Yasuda, T. (1977). Mossy fibre and climbing fibre responses produced in the cerebellar cortex by stimulation of the cerebral cortex in monkeys. *Experimental Brain Research, 29,* 419–428.

Schmahmann, J. D., Doyon, J., McDonald, D., Holmes, C., Lavoie, K., Hurwitz, A. S., et al. (1999). Three-dimensional MRI atlas of the human cerebellum in proportional stereotaxic space. *Neuroimage, 10,* 233–260.

Schmid, A., Rees, G., Frith, C., & Barnes, G. (2001). An fMRI study of anticipation and learning of smooth pursuit eye movements in humans. *NeuroReport, 12,* 1409–1414.

Schlag, J., & Schlag-Rey, M. (1987). Evidence for a supplementary eye field. *Journal of Neurophysiology, 57,* 179–200.
Sherrington, C. S. (1918). Observations on the sensual role of the proprioceptive nerve supply of the extrinsic ocular muscles. *Brain, 41,* 332–343.
Shipp, S., Blanton, M., & Zeki, S. (1998). A visuo-somatomotor pathway through superior parietal cortex in the macaque monkey: Cortical connections of areas V6 and V6a. *European Journal of Neuroscience, 10,* 3171–3193.
Shook, B. L., Schlag-Rey, M., & Schlag, J. (1990). Primate supplementary eye field: I. Comparative aspects of mesencephalic and pontine connections. *The Journal of Comparative Neurology, 301,* 618–642.
Sperry, R. W. (1950). Neural basis of the spontaneous optokinetic response produced by visual inversion. *Journal of Comparative and Physiological Psychology, 43,* 482–489.
Sunaert, S., van Hecke, P., Marchal, G., & Orban, G. A. (1999). Motion-responsive regions of the human brain. *Experimental Brain Research, 127,* 355–370.
Tanabe, J., Tregellas, J., Miller, D., Ross, R. G., & Freedman, R. (2002). Brain activation during smooth-pursuit eye movements. *Neuroimage, 17,* 1315–1324.
Thier, P., & Erickson, R. G. (1992). Response of visual-tracking neurons from cortical area MST-l to visual, eye and head motion. *European Journal of Neuroscience, 4,* 539–553.
Thier, P., Haarmeier, T., Chakraborty, S., Lindner, A., & Tikhonov, A. (2001). Cortical substrates of perceptual stability during eye movements. *Neuroimage, 14,* S33–S39.
Thilo, K. V., Probst, T., Bronstein, A. M., Ito, Y., & Gresty, M. A. (1999). Torsional eye movements are facilitated during perception of self-motion. *Experimental Brain Research, 126,* 495–500.
Tikhonov, A., Haarmeier, T., Thier, P., Braun, C., & Lutzenberger, W. (2004). Neuromagnetic activity in medial parieto-occipital cortex reflects the perception of visual motion during eye movements. *Neuroimage, 21,* 593–600.
von Helmholtz, H. (1962). *Physiological optics Vol. III.* Translated from the 3rd German edition of 1910. New York: Dover.
von Holst, E., & Mittelstaedt, H. (1950). Das Reafferenzprinzip. *Naturwissenschaften, 37,* 464–476.
Wertheim, A. H. (1994). Motion perception during self-motion: The direct versus inferential theory revisited. *Behavioral and Brain Science, 17,* 293–355.
Zald, D. H., Donndelinger, M., & Pardo, J. V. (1998). Elucidating dynamic brain interactions with across-subjects correlational analyses of positron emission tomographic data: The functional connectivity of the amygdala and orbitofrontal cortex during olfactory tasks. *Journal of Cerebral Blood Flow and Metabolism, 18,* 896–905.